

Hydrothermal synthesis of Ni₂P nanoparticle and its hydrodesulfurization of dibenzothiophene

Qi Zhao · Yang Han · Xiang Huang · Jinhui Dai ·
Jintao Tian · Zhibin Zhu · Li Yue

Received: 12 October 2016 / Accepted: 7 February 2017 / Published online: 24 March 2017
© Springer Science+Business Media Dordrecht 2017

Abstract Nanosized nickel phosphide (Ni₂P) has been synthesized via hydrothermal reaction with environmental-friendly red phosphorus and nickel chloride. The reaction mechanism has been studied by measurement techniques of IC, XRD, TEM, EDS, and XPS. The results showed that the particle sizes of as-prepared Ni₂P are in nanoscale ranging from 10 to 30 nm. In hydrothermal reaction, red phosphorus reacts with water to its oxyacids, especially its hypophosphorous acid (or hypophosphite) which can reduce nickel chloride to nickel, and then metallic nickel will penetrate into the rest of red phosphorus to generate nano-Ni₂P. Furthermore, the catalytic performance of as-synthesized Ni₂P for the hydrodesulfurization of dibenzothiophene has been tested. It has been shown that the HDS reaction process over Ni₂P catalyst agrees well with the pseudo-first order kinetic equation, and the HDS conversion can reach up to 43.83% in 5 h with a stable increasing catalytic activity during the whole examination process.

Keywords Hydrothermal synthesis · Red phosphorus · Oxyacid · Nickel · Nanometer · HDS

Introduction

Nickel phosphide has a variety of phases, in which Ni₂P is a kind of material with excellent corrosion resistance, wear resistance, and oxidation resistance. The nano-crystal of Ni₂P has good plasticity, toughness, and higher specific heat, making it adaptable for a variety of carriers as the catalytic center (Wu et al. 2013; Song et al. 2010; Koranyi et al. 2009). At the same time, because of its special intrinsic high catalytic activity and selective hydrogenation such as high desulfurization, carbon deposition resistance, resistance to poisoning, and so on (Zhang et al. 2011), Ni₂P also overcomes the weakness of low stability of the traditional catalyst (Savithra et al. 2013), which makes it to have higher HDS activity than a sulfide catalyst (Duan et al. 2009). The Ni₂P catalyst is possibly a new catalytic material which can replace the traditional sulfide catalysts and becomes the hotspot of current research on hydrodesulfurization (Song et al. 2012a, b).

At present, the main preparation methods of Ni₂P used as a catalyst are as follows (Song et al. 2007; Wang et al. 2009; Muthuswamy and Savithra 2011; Cecilia et al. 2009; Chen et al. 2010): (1) direct combination of metal nickel and red phosphorus under high temperature and protective atmosphere, (2) solid phase reaction of halogenated nickel and phosphorus, (3) reaction of nickel salt and phosphine, (4) decomposition of organic nickel compounds, (5) molten electrolysis of nickel salt, (6) reduction of phosphate containing nickel, etc. But most of these preparation methods need high temperature and high pressure, and some of them still need very expensive or dangerous materials; many

Q. Zhao · Y. Han · X. Huang (✉) · J. Dai · J. Tian ·
Z. Zhu · L. Yue
Institute of Materials Science and Engineering, Ocean University
of China, No. 238 Songling Road, Qingdao 266100, People's
Republic of China
e-mail: materials@ouc.edu.cn

reactions even use highly toxic substances such as phosphine as phosphorus source.

Therefore, hydrothermal (solvothermal) synthesis methods of phosphides developed in recent years (Kirill et al. 2006; Jennifer et al. 2005; Liu et al. 2007; Huang et al. 2012; Wang et al. 2013; Huang et al. 2013; Huang et al. 2014; Liu et al. 2010), utilizing the disproportionation reaction of elemental phosphorus (especially non-toxic red phosphorus) in the water (solvent) (Jiang and Shen 2000), is both simple in preparation as well as causing less environmental concerns. With the rising conflict between petroleum deterioration and environmental protection, the extensive and in-depth exploration of the synthesis process, phase structure, surface properties, and catalytic performance of Ni₂P prepared by hydrothermal method will become the hot focus. The most basic synthesis reaction process will fully demonstrate the important significance of theoretical research and potential application prospects of this new catalytic material. But up till now, little work has been done on the reaction mechanism and HDS performance of Ni₂P nanoparticle prepared by hydrothermal method (Christos et al. 2016; Sophie et al. 2013).

In this study, we reported a synthesis mechanism of Ni₂P nanoparticle via hydrothermal route using nontoxic red phosphorus and nickel chloride. The process was concise and environmental. Furthermore, the catalytic performance of the as-synthesized Ni₂P in dibenzothiophene hydrodesulfurization (HDS) was examined.

Experimental

Chemicals

All chemicals involved in the experiments were analytical reagents: Red phosphorus (P), nickel chloride (NiCl₂·6H₂O), potassium hydroxide (KOH), ZSM-5, dibenzothiophene (C₁₂H₈S) (Aladdin, AR standard), and decahydronaphthalene (C₁₀H₁₈) (Sinopharm, AR standard).

Synthesis of materials

Hydrothermal treatment of red phosphorus

The hydrothermal treatment process of red phosphorus was carried out as follows: First, red phosphorus (6.2 g) was ground for 20 min with 20 ml water in a mortar. Then, the mixture was transferred into a Teflon-lined stainless

steel autoclave with 40 ml distilled water to make sure that the filling factor was 80% and heated at 200 °C for 10 h. After the autoclave cooled to room temperature, the filtrate L₁ of hydrothermal red phosphorus was obtained; Finally, the filtrate L₁ (60 ml) was heated again at 200 °C for 10 h to get the liquid L₂.

Hydrothermal synthesis of nano-Ni₂P

The hydrothermal synthesis of nano-Ni₂P was carried out as follows: First, NiCl₂·6H₂O (1.91 g) was mixed in the filtrate L₁ (60 ml). The mixture was adjusted to pH = 13 with 1 mol/L KOH solution, then the green suspension liquid was transferred into a Teflon-lined stainless autoclave and heated at 200 °C for 5 h. Finally, when the autoclave cooled to room temperature, the powder A was separated by vacuum filtration, rinsed repeatedly with distilled water, and then dried at 60 °C for 3 h. To investigate the synthesis mechanism of Ni₂P via hydrothermal route, red phosphorus (6.2 g) obtained by the first step was put to NiCl₂·6H₂O (1.91 g) solution and adjusted to pH = 13; then the mixture was transferred into a Teflon-lined stainless steel autoclave and heated at 200 °C for 5 and 10 h, respectively. The as-prepared powder B and powder C were collected by vacuum filtration, rinsed repeatedly with distilled water and then dried at 60 °C for 3 h.

Hydrothermal synthesis of supported Ni₂P/ZSM-5

The hydrothermal synthesis of supported Ni₂P/ZSM-5 was carried out as follows: First, red phosphorus (6.2 g) of hydrothermal treatment was mixed with NiCl₂·6H₂O (1.91 g) in a beaker with 60 ml distilled water, then ZSM-5 (2.4 g) were added to the mixed aqueous suspension under vigorous electromagnetic stirring, and the mixture was adjusted to pH = 13 with 1 mol/L KOH solution. Finally, the mixture was transferred into a 80 ml Teflon-lined stainless steel autoclave (filling ratio:80%) and heated at 200 °C for 10 h. The as-prepared powder D was collected by vacuum filtration, rinsed repeatedly with distilled water, and then dried at 60 °C for 3 h. In a typical synthesis experiment, red phosphorus was excess, and the upper solution after hydrothermal process was clear and colorless, proving that the nickel elements were totally consumed and converted into nickel phosphide (Ni₂P). Based on this fact, the weight of the Ni₂P in Ni₂P/ZSM-5 system was calculated according to the quality of the nickel element in nickel chloride (NiCl₂·6H₂O).

Characterization and test

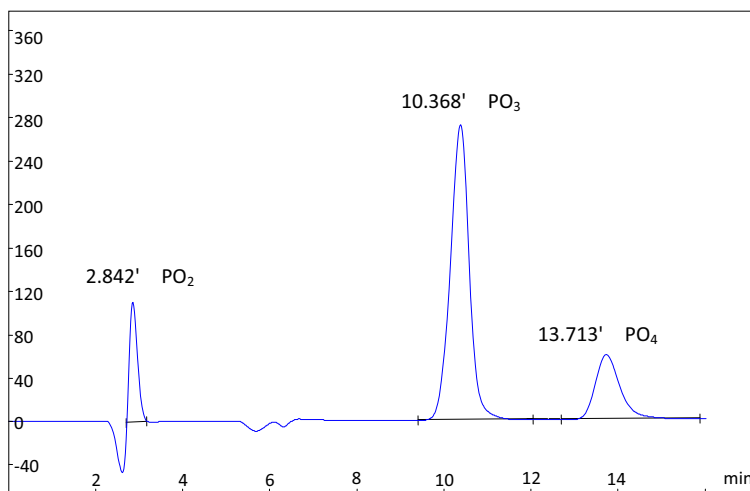
Characterization analysis

The concentration of various radicals were tested by ion chromatography (IC; Model PIC-10A (120255), Puren Instrument Co., Qingdao) which used YSA (001) as chromatographic column. The XRD patterns were recorded on a Bruker AXS-D8 Advance powder diffractometer with a Cu K α radiation source, and the XRD patterns were collected at 40 Kv and 40 mA with a scanning rate of 5°/min from 20 to 90°. A JEM-1200EX (JEOL Co, Japan) transmission electron microscope was operated at 100 kV to obtain TEM images, and the EDS spectrum was collected using Oxford Instruments' INCA EDS system. The XPS on Ni₂P catalyst was obtained with an ESCALAB 250Xi Termo spectrometer equipped with a monochromatic X-ray source Al K α under ultra-high vacuum and a hemispherical analyzer.

HDS reaction tests

The activity tests were carried out in a 100 ml stainless steel autoclave with mechanical stirring. The decahydronaphthalene solution containing 0.03 wt% (sulfur content) dibenzothiophene was selected as model reactant. In a typical experiment, 40.0 g of dibenzothiophene solution was charged into the reactor, together with 0.4 g of the Ni₂P catalyst. Prior to the reaction, the reactor was purged three times with H₂ to exchange the air inside. The reaction was carried out at 300 °C and 2.0 MPa H₂ (initial pressure at room temperature) for different times (1 ~ 4 h)

Fig. 1 Ion chromatogram of filtrate L₁ (red phosphorus + water, 200 °C, 10 h, diluted 50-fold)



with a stirring rate of 500 r min⁻¹. The liquid product was collected by centrifugation and analyzed on an Agilent 7890 GC-MS instrument equipped with a HP-5MS column. The desulfurization efficiency of DBT is calculated by the following formula:

$$\text{HDS}\% = \left(1 - \frac{\text{final total surful content}}{\text{initial total surful content}} \right) \times 100\%$$

Results and discussions

Hydrothermal treatment of red phosphorus

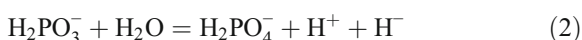
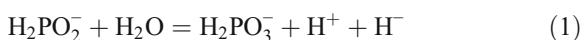
The ion chromatogram of filtrate L₁ diluted 50-fold is shown in Fig. 1. Table 1 presents the concentration of various phosphorus radicals in filtrate L₁. In hydrothermal reaction, red phosphorus reacts with water to form its oxyacids, including hypophosphorous acid, phosphorous acid, and phosphoric acid (Yao et al. 1998). The pH value of filtrate L₁ is 1 ~ 3. Fig. 2 is the ion chromatograph of L₂ diluted 1000-fold obtained by hydrothermal treatment of filtrate L₁. The re-hydrothermal solution L₂ is still clear. The concentration of different phosphorus ionic groups in liquid L₂ are displayed in Table 2. The pH value of liquid L₂ increases slightly to 2 ~ 4.

Comparing Table 1 and Table 2, it can be found that the hypophosphorous acid in the liquid L₂ disappears, the concentration of phosphorous acid decreases, and the concentration of phosphoric acid increases, which indicates that the hypophosphorous acid will further convert to phosphorous acid and phosphoric acid under hydrothermal condition, and the reaction is quick

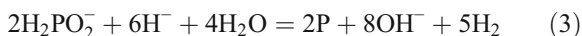
Table 1 IC test results of filtrate L₁

Name	Retention time (min)	Concentration (mg/L)	Peak area	Original concentration (mg/L)
PO ₂	2.842	20.99	1,400,394	1049
PO ₃	10.368	35.52	8,219,120	1776
PO ₄	13.713	16.1	2,378,360	805

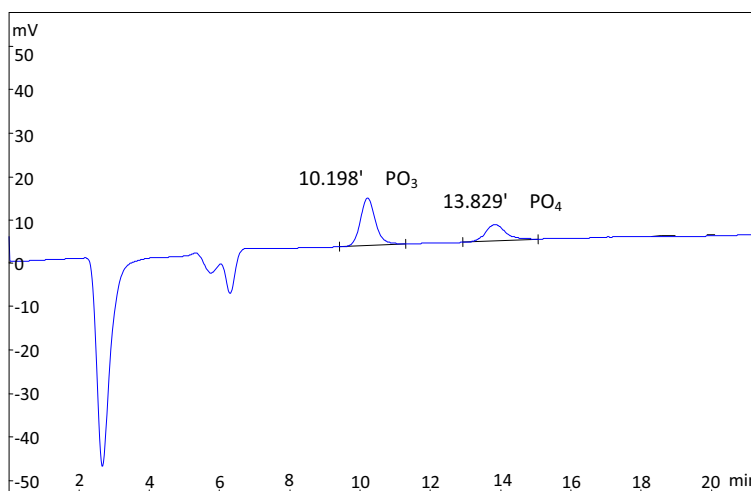
(complete transformation of hypophosphorous acid); the phosphorous acid also can be converted to phosphoric acid, but the reaction is relatively slow (partial conversion of phosphorous acid). According to Hydride Transfer Theory proposed by Hersch (Jiang and Shen 2000), hypophosphorous acid can react with water to generate phosphorous acid in acidic medium; meanwhile, phosphorous acid also can react with water to generate phosphoric acid, i.e.,



The explanation of eutectoid phosphorus is as below:



The Eqs. (1)~(3) can explain that the hypophosphorous acid in liquid L₂ disappears, the concentration of phosphorous acid decreases, and the concentration of phosphoric acid increases. While, the Eq. (3) can explain the reduce of the total phosphorus content in the solution.

Fig. 2 Ion chromatogram of clarified liquid L₂ (filtrate, 200 °C, 10 h, diluted 1000-fold)**Table 2** IC test results of clarified liquid L₂

Name	Retention time (min)	Concentration (mg/L)	Peak area	Original concentration (mg/L)
PO ₃	10.198	1.348	334,858	1348
PO ₄	13.829	1.067	166,010	1067

Hydrothermal synthesis of nano-Ni₂P

Fig. 3 shows the X-Ray diffraction patterns of the hydrothermal products. From Fig. 3a, the diffraction peaks of the powder A are readily indexed to a crystalline phase of Ni (PDF# = 70–1849) which is strongly magnetic. When the red phosphorus of hydrothermal treatment replaces the filtrate L₁, the peak intensity of Ni is weakened and peaks become wider obviously (Fig. 3b). In addition, the diffraction peaks of Ni₂P (PDF# = 74–1385) appear and the mixture is weakly magnetic. Nevertheless, with the duration rising up to 10 h, the diffraction peaks completely change to Ni₂P (PDF# = 74–1385, Fig. 3c) in which there is no magnetism.

Combining Figs. 1 and 3a, it is known that the filtrate L₁ (especially the hypophosphorous acid which has a strong reducibility) will reduce NiCl₂ to metallic nickel in hydrothermal conditions. After the autoclave is cooled to room temperature, the inner liner still retains a great residual pressure and gives off a certain amount of colorless and tasteless gas H₂ (Cl and P are basically excluded, the reaction system of the solution has a strong reducibility and does not readily generate O₂, so the resulting gas is H₂). In addition to a small amount of

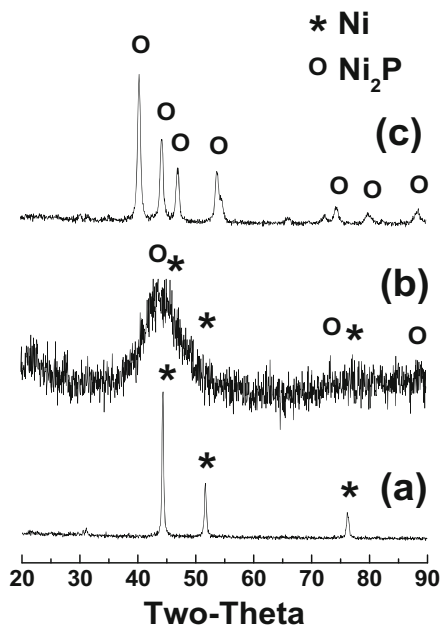
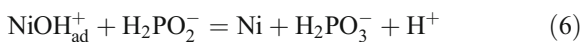
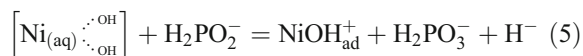
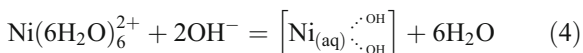


Fig. 3 XRD patterns of hydrothermal products. **a** Powder A(Ni) (filtrate L₁ + NiCl₂•6H₂O, pH = 13, 200 °C, 10 h). **b**: Powder B(Ni + Ni₂P) (P + NiCl₂•6H₂O, pH = 13,200 °C,5 h). **c** Powder C(Ni₂P) (P + NiCl₂•6H₂O, pH = 13, 200 °C, 10 h)

precipitated powder A (Ni) in the inner liner, there also remain many powders of A (Ni) tightly adhered to the inner wall and the bottom, which is difficult to remove. As the initial system is adjusted to alkalinity, the nickel source of the reaction is Ni (OH)₂, which is in accordance with the theory of the distribution of hydroxyl and nickel ions in chemical plating (Hersch 1955; Meeradder 1981; Jiang and Shen 2000; Stojan 2002; Zhang et al. 2013). The reaction mechanism is as below:



For the reactions generating the powder B and C, after the autoclaves cooled to room temperature, both of them still remain a high pressure and give off a lot of colorless and tasteless gas. A layer of the powder B (or C) is

closely adhered to the inner wall and the bottom, and a large number of white bubbles are attached at the same time. Compared to the powder A, there is a sufficient amount of red phosphorus to provide sufficient hypophosphorous acid (or hypophosphite) for the following reaction (5) ~ (6). Therefore, the gas production increases; the inner wall and the bottom are completely black (adhesive powder B or C) with many white bubbles attached to them. It can further indicate that in the process of preparing Ni₂P with red phosphorus as the source of phosphorus via the hydrothermal method, red phosphorus will not directly react with NiCl₂, but the hypophosphorous acid with strong reducibility generated by the reaction of red phosphorus and water reduces the nickel source to metallic nickel. The generated nickel reacts with the rest of red phosphorus to produce Ni₂P:



Therefore, the Eqs. (4) ~ (7) and (8) are the main reactions to prepare Ni₂P with hydrothermal red phosphorus as phosphorus material via hydrothermal synthesis.

XPS spectra of Ni 2p and P 2p region of as-synthesized Ni₂P were obtained for the analyzing the surface elemental composition and valence state of the Ni₂P sample (Fig. 4). The Ni 2p_{3/2} spectrum (Fig. 4a) shows three peaks at 853.8, 856.7, and 862.1 eV which can be assigned to NiO, Ni²⁺ and the satellite of the Ni 2p_{3/2} peak (Ai et al. 2008; Ma et al. 2009; Yang et al. 2010), respectively. The P 2p spectrum (Fig. 4b) shows two peaks at 129.7 and 130.8 eV corresponding to the P 2p_{3/2} and P 2p_{1/2} in Ni₂P, respectively (Li et al. 2015). Furthermore, the spectrum of P 2p also exhibits a peak at 133.7 eV, which can be attributed to oxidized P species formed on the surface of Ni₂P due to air contact (Chen et al. 2009).

Fig. 5 shows the transmission electron microscopy (TEM) images of the hydrothermal products. It can be observed that the particle sizes of the powders A (Ni), B (Ni and Ni₂P), C (Ni₂P), and the red phosphorus (P) of hydrothermal treatment are all below 50 nm. Furthermore, the sizes of the powder A, B, and C (10 ~ 30 nm) calculated by Scherrer equation and the TEM results are in close agreement with each other. Namely, the synthesis technique of Ni₂P via hydrothermal method with red phosphorus of hydrothermal treatment as phosphate source is simple and easy to control, the raw materials are cheap, and the particle size of Ni₂P is at the nanometer level (Fig. 6).

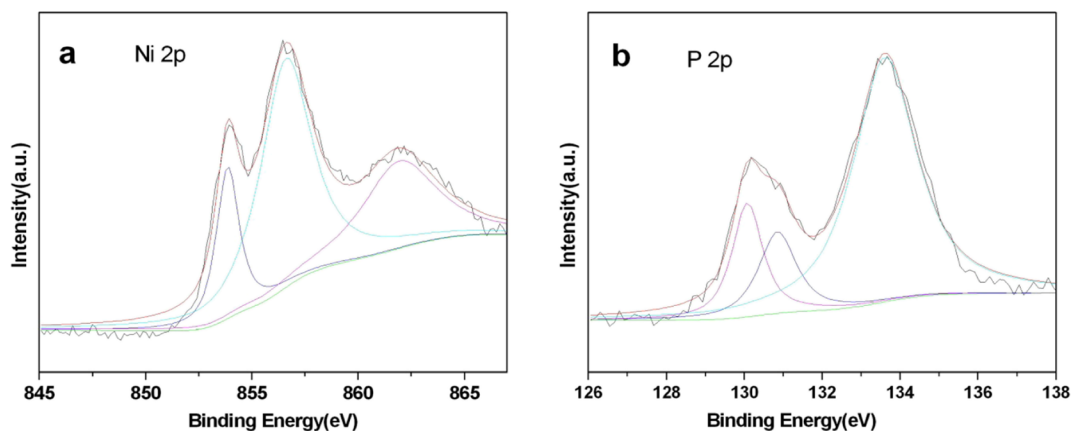


Fig. 4 XPS spectra of **a** Ni 2p and **b** P 2p from Ni₂P sample

HDS activity tests

The HDS activity tests are conducted in an autoclave reactor by using dibenzothiophene as a model S-containing compound over the as-prepared Ni₂P catalyst. Table 3 is the HDS results of Ni₂P catalysts with different reaction times.

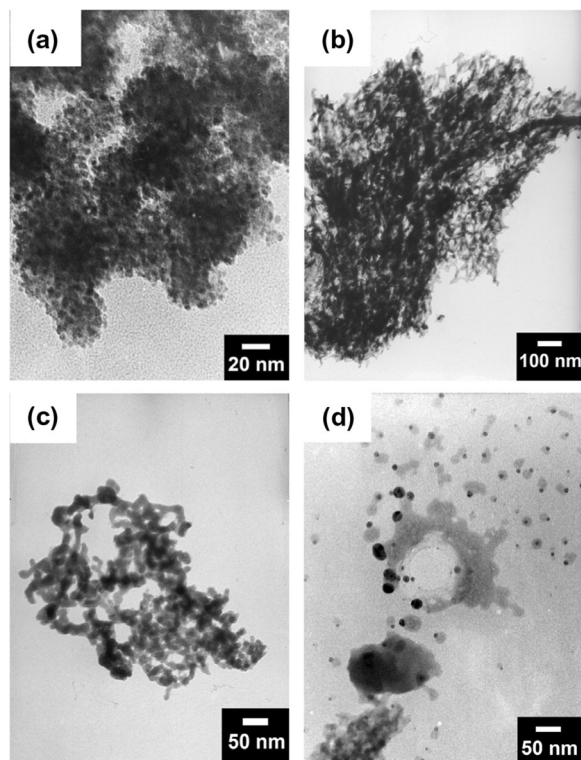


Fig. 5 TEM micrographs of hydrothermal products. **a** Powder A (Ni). **b** Powder B (Ni + Ni₂P). **c** Powder C (Ni₂P). **d** Red phosphorus of hydrothermal treatment (pH = 13, 200 °C, 10 h)

Generally, the HDS of DBT undergoes two parallel routes involving direct desulfurization (DDS) and hydrodesulfurization (HYD) (Al-Rashidy et al. 2015). The DDS route mainly leads to the formation of biphenyl because of direct C–S bond rupture, while the HYD route mainly leads to the formation of cyclohexylbenzene through a hydrogenation–desulfurization process. The selectivity results (Table 3) show that the selectivity of Cyclohexylbenzene is increasing while the selectivity of Biphenyl is declining with the prolonging of reaction time. This may be because there are two types of sites in Ni₂P, Ni(1) site with quasi tetrahedral coordination and Ni(2) sites with square pyramidal coordination. Ni(1) site is likely involved in the DDS while Ni(2) site is responsible for the high catalytic activity in the HYD pathway in the HDS reaction (Oyama and Lee 2008; Song et al. 2012a, b).

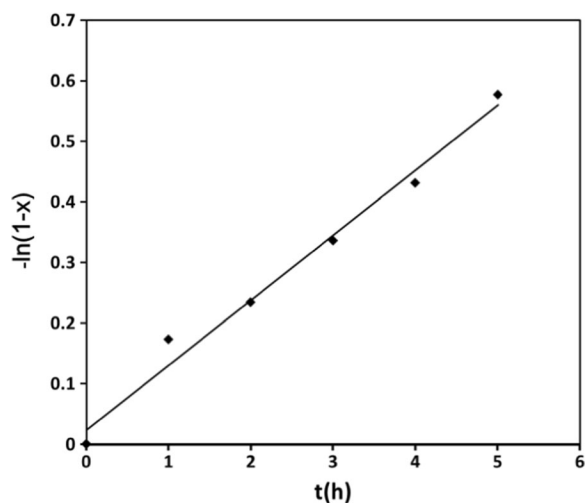
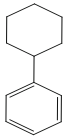
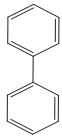


Fig. 6 First order-fitting diagram of different HDS times vs. corresponding conversion

Table 3 The results of HDS test of Ni₂P

Catalysts	HDS test time (h)	Selectivity to the products (wt.%)		Conversion (wt.%)	Rate constant (h ⁻¹)
					
		Cyclohexylbenzene	Biphenyl		
Ni ₂ P-1	1	25	75	15.89	0.173
Ni ₂ P-2	2	27.78	72.22	20.93	0.117
Ni ₂ P-3	3	28.57	71.43	28.57	0.112
Ni ₂ P-4	4	29.17	70.83	35.04	0.108
Ni ₂ P-5	5	42.25	57.75	43.83	0.115
Ni ₂ P-old	4	34.55	65.45	31.43	0.094
Ni ₂ P/ZSM-5	4	45.45	54.55	31.25	0.094
ZSM-5	4	0	0	0	0

(Ni₂P-*n* the Ni₂P with different HDS reaction times, Ni₂P-old the catalyst sample placed in air for 2 months)

Hence, the acceleration of the HYD pathway must be associated with the increasing amount of Ni(2) sites while the number of Ni(1) sites remains unchanged (Song et al. 2014). As shown in Table 3, the conversion of Ni₂P placed in air for 2 months is 31.25% which is almost unchanged compared with fresh Ni₂P. However, the conversion of supported Ni₂P/ZSM-5 is 31.25% similar to unsupported Ni₂P. Indeed, though supported catalysts should have a greater catalytic efficiency for a greater specific surface area and more active centers are exposed, the load rate of supported Ni₂P/ZSM-5 is only 20% in this paper. Besides, the quality of the catalysts (Ni₂P catalyst or supported Ni₂P/ZSM-5 catalyst) used are equal in the HDS test process. Therefore, the conversion of supported Ni₂P/ZSM-5 we obtained is not ideal. This may be due to an increase in specific surface area, but the total content of catalyst decreased.

According to Table 3, the first order fitting diagram of different HDS test times can be drawn. We can obtain an inclined straight line nearly through the origin with time (*t*) as the abscissa and $-\ln(1-x)$ as the ordinate as shown in Fig. 5, which according to pseudo-first order kinetic equation,

$$-\ln(1-x) = kt$$

The rate constant (*k*) of this reaction is about 0.1. (*x*, desulfurization conversion; *t*, HDS test time; *k*, rate constant).

Fig. 7 shows the X-Ray diffraction patterns of Ni₂P before and after the HDS test. With the different HDS reaction time, all the diffraction peaks can be indexed to the crystalline phase of Ni₂P (PDF# = 74-1385) before and after HDS test (Fig. 7 (a) ~ (f)), which shows that the Ni₂P catalyst is stable in the HDS reaction.

The EDS spectrum of Ni₂P-old, fresh Ni₂P powders, and Ni₂P after HDS test in Fig. 8a-c shows that the presence of Ni and P in the products, and the Ni/P ratio is equal to about 2.3:1, 2.7:1, and 2.5:1, respectively.

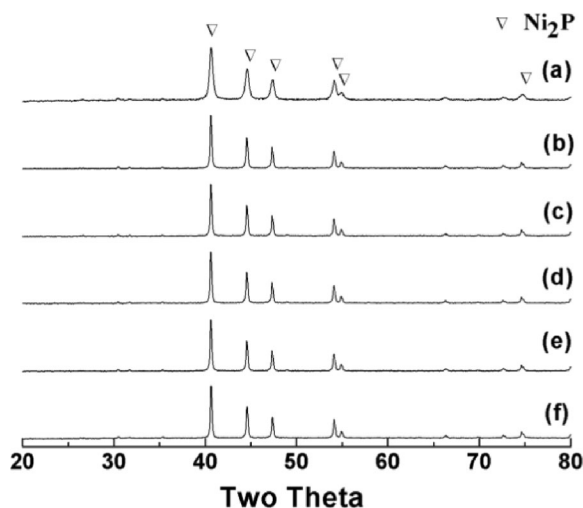
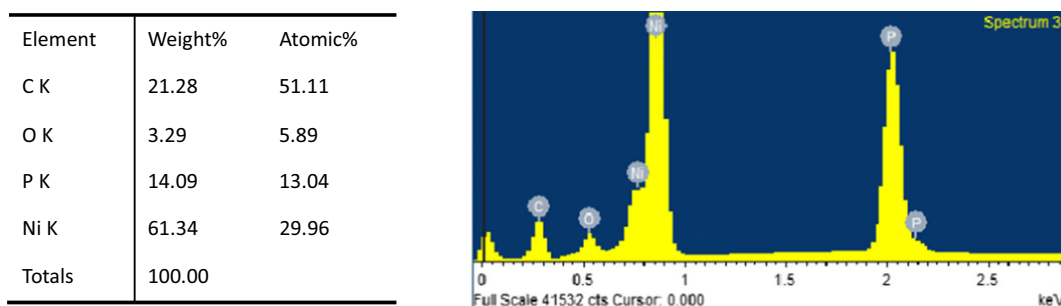
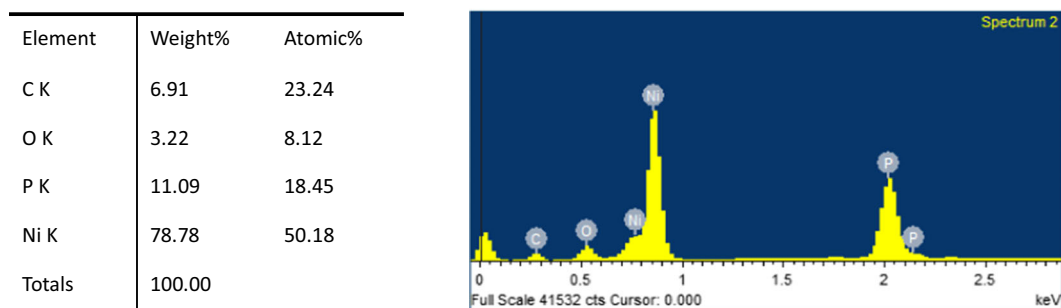


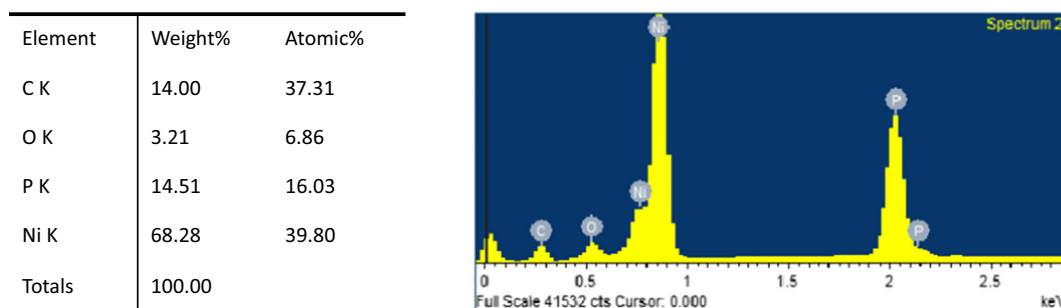
Fig. 7 XRD patterns of Ni₂P before and after HDS test. **a** Ni₂P before HDS test. **b** 1 h HDS test of Ni₂P. **c** 2 h HDS test of Ni₂P. **d** 3 h HDS test of Ni₂P. **e** 4 h HDS test of Ni₂P. **f** 5 h HDS test of Ni₂P



a EDS spectra of Ni₂P-old powders (Ni:P=29.96:13.04=2.3:1)



b EDS spectra of fresh Ni₂P powders (Ni:P=50.18:18.45=2.7:1)



c EDS spectra of Ni₂P after HDS test (Ni:P=39.80:16.03=2.5:1)

Fig. 8 **a** EDS spectra of Ni₂P-old powders (Ni:P = 29.96:13.04 = 2.3:1). **b** EDS spectra of fresh Ni₂P powders (Ni:P = 50.18:18.45 = 2.7:1). **c** EDS spectra of Ni₂P after HDS test (Ni:P = 39.80:16.03 = 2.5:1)

The results once again indicate that the Ni₂P catalyst is very stable before and after HDS reaction.

Conclusions

In this work, the reaction mechanism of Ni₂P via hydrothermal synthesis is studied, and the as-synthesized products' catalytic performances are examined in dibenzothiophene hydrodesulfurization

reaction. Some conclusions from this study are summarized below:

- 1) The reaction mechanism of Ni₂P via hydrothermal synthesis is as follows: Firstly, red phosphorus (P) reacts with water to its oxyacids. Then strong reducibility of hypophosphorous acid (or hypophosphite) can reduce nickel chloride to metal nickel accompanying the generation of H₂ gas. Finally, the metallic nickel reacts with the rest of the red phosphorus to produce Ni₂P.

- 2) The particle sizes of red phosphorus (P) after hydrothermal treatment are in nano-level (10 ~ 30 nm), and the particle sizes of Ni₂P with the as-obtained nano red phosphorus as raw material are also in nanoscale.
- 3) The Ni₂P catalyst in the process of HDS test meets to the pseudo-first order kinetic equation.
- 4) The stability of Ni₂P active center during HDS performance test is excellent.

Acknowledgements Financial support from the Natural Science Foundation of Shandong Province of China (No.ZR2014BM022) is gratefully acknowledged.

Compliance with ethical standards

Conflict of interest The authors declare that they have no conflict of interest.

References

- Ai L, Fang GJ, Yuan LY, Liu NS (2008) Influence of substrate temperature on electrical and optical properties of p-type semitransparent conductive nickel oxide thin films deposited by radio frequency sputtering. *Appl Surf Sci* 254:2401–2405
- Al-Rashidy AH, Ali SA, Ahmed S, Razzak SA, Hossain MM (2015) Phenomenological kinetics modeling of simultaneous HDS of dibenzothiophene and substituted dibenzothiophene over CoMoP/Al₂O₃ catalysts. *Chem Eng Res Des* 104:819–827
- Cecilia JA, Infantes-Molina A, Rodríguez-Castellón E (2009) A novel method for preparing an active nickel phosphide catalyst for HDS of dibenzothiophene. *J Catal* 263(1):4–15
- Chen YZ, She HD, Luo XH, Yue GH (2009) Solution-phase synthesis of nickel phosphide single-crystalline nanowires. *Journal of Crystal Growth* 311:1229–1233
- Chen JX, Chen Y, Yang Q (2010) An approach to preparing highly dispersed Ni₂P/SiO₂ catalyst. *Catal Commun* 11(6):571–575
- Christos K, Kyriakos B, Mantha G (2016) Development of nickel based catalysts for the transformation of natural triglycerides and related compounds into green diesel: a critical review. *Appl Catal B Environ* 181:156–196
- Duan XP, Teng Y, Wang AJ (2009) Role of sulfur in hydrotreating catalysis over nickel phosphide. *J Catal* 261(2):232–240
- Hersch P. (1955-1956) *Trans Inst Met Finish* 33:417–422
- Huang H, Huang X, Zhu ZB, Dai JH (2012) Hydrothermal synthesis of cobalt phosphide nanoparticles. *Ceram Int* 38:1713–1715
- Huang X, Sun JJ, Wang B, Huang H (2013) A novel solvothermal route to nanocrystalline Sn₄P₃ with red phosphorous as raw material. *Adv Mater Res* 704:241–245
- Huang X, Dong Q, Huang H, Yue L, Zhu ZB, Dai JH (2014) Facile synthesis of iron phosphide Fe₂P nanoparticle and its catalytic performance in thiophene hydrodesulfurization. *J Nanopart Res* 16:2785
- Jennifer AA, Valentina GH, Stephanie LB (2005) Solvothermal syntheses of Cu₃P via reactions of amorphous red phosphorus with a variety of copper sources. *J Solid State Chem* 178: 970–975
- Jiang XX, Shen W (2000) *The fundamental and practice of electroless plating*. National Defence Industry Press, Beijing, pp 12–20
- Kirill AK, Yury VK, Sugata R (2006) A facile high-yield solvothermal route to tin phosphide Sn₄P₃. *J Solid State Chem* 179:3756–3762
- Koranyi TI, Coumans AE, Hensen EJM (2009) The influence of metal loading and activation on mesoporous materials supported nickel phosphide hydrotreating catalysts. *Appl Catal A Gen* 365(1):48–54
- Li JY, Zhou XM, Xia ZM, Zhang ZY (2015) Facile synthesis of CoX(X=S, P) as an efficient electrocatalyst for hydrogen evolution reaction. *J Mater Chem A* 3:13066–13071
- Liu SL, Liu XZ, Xu LQ (2007) Controlled synthesis and characterization of nickel phosphide nanocrystal. *J Cryst Growth* 304(2):430–434
- Liu ZY, Huang X, Zhu ZB (2010) A simple mild hydrothermal route for the synthesis of nickel phosphide powders. *Ceram Int* 36(3):1155–1158
- Ma Z, Wang JB, Liu QF, Yuan J (2009) Microwave absorption of electroless Ni–Co–P-coated SiO₂ powder. *Appl Surf Sci* 255: 6629–6623
- Meeradder JEAMVD (1981) On the mechanism of electroless plating. II. One mechanism for different reductants. *J Appl Electrochem* 11:395–400
- Muthuswamy E, Savithra GHL (2011) Brock Stephanie L, synthetic levers enabling independent control of phase, size, and morphology in nickel phosphide nanoparticles. *ACS Nano* 5(3):2402–2411
- Oyama ST, Lee YK (2008) The active site of nickel phosphide catalysts for the hydrodesulfurization of 4,6-DMDBT. *Catalysis* 258:393–400
- Savithra GHL, Bowker RH, Carrillo Bo A (2013) Rational design of nickel phosphide hydrodesulfurization catalysts: controlling particle size and preventing sintering. *Chem Mater* 25(6):825–833
- Song LM, Li W, Zhang MH (2007) Preparation and characterization of Ni₂P/SiO₂-Al₂O₃ and its catalytic performance for hydrodesulfurization of 4, 6- Dimethyldibenzothiophene. *Chin J Catal* 28(2):143–147
- Song H, Guo YT, Li F (2010) Preparation, hydrodesulfurization and hydrodenitrogenation performance of a Ni₂P/TiO₂-Al₂O₃ catalyst. *Acta Phys -Chim Sin* 26(9):2461–2467
- Song H, Dai M, Guo YT (2012a) Preparation of composite TiO₂-Al₂O₃ supported nickel phosphide hydrotreating catalysis and catalytic activity for hydrodesulfurization of dibenzothiophene. *Fuel Process Technol* 96:228–236
- Song H, Dai M, Song HL (2012b) Ni₂P catalyst for hydrodesulfurization. *Progress In Chemistry* 24:757–767
- Song H, Wang J, Wang ZD, Song HL (2014) Effect of titanium content on dibenzothiophene HDS performance over Ni₂P/Ti-MCM-41 catalyst. *J Catal* 311:257–265
- Sophie C, David P, Cédric B (2013) Nanoscaled metal borides and phosphides: recent developments and perspectives. *Chem Rev* 113(10):7981–8065

- Stojan SD (2002) Electroless deposition of metals and alloys. *Modern Aspects of Electrochemistry* 35:51–133
- Wang JW, Johnston-Peck AC, Tracy JB (2009) Nickel phosphide nanoparticles with hollow, solid, and amorphous structures. *Chem Mater* 21(19):4462–4467
- Wang B, Huang X, Zhu ZB, Huang H, Dai JH (2013) Hydrothermal synthesis of nano nickel phosphides and investigation of their thermal stability. *Int J Mater Res* 104: 507–510
- Wu SK, Lai PC, Lin YC (2013) Atmospheric hydrodeoxygenation of guaiacol over alumina-, zirconia-, and silica-supported nickel phosphide catalysts. *ACS Sustain Chem Eng* 1(3): 349–358
- Yang RC, Wu JS, Li XG (2010) Hydrotreating of crude 2-ethylhexanol over Ni/Al₂O₃ catalysts: influence of the Ni oxide dispersion on the active sites. *Applied Catalysis A* 383:112–118
- Yao SZ, Zhu YB, He SE, Nie LH (1998) *Handbook of chemical reactions of elements*. Hunan Education Press, Changsha, pp 383–386
- Zhang YJ, Song H, Jiang SR (2011) Progress of research on factors affecting HDS catalyst activity. *Advances In Fine Petrochemical* 12(10):23–30
- Zhang BW, Liao SZ, Xie HW, Zhang H (2013) Progress of electroless amorphous and nanoalloy deposition: a review—part 1. *Transactions of the IMF* 91:310–318